

Overtone spectroscopy of  $\text{H}_2\text{D}^+$  and  $\text{D}_2\text{H}^+$  using laser induced reactionsOskar Asvany<sup>a)</sup>*Raymond and Beverly Sackler Laboratory for Astrophysics, Leiden Observatory, P.O. Box 9513, 2300 RA Leiden, The Netherlands*

Edouard Hugo

*I. Physikalisches Institut, Universität zu Köln, Zùlpicher Strasse 77, 50937 Köln, Germany*Frank Müller<sup>b)</sup>*Institut für Angewandte Physik, Universität Bonn, Wegelerstrasse 8, 53115 Bonn, Germany*

Frank Kühnemann

*Physics Department, German University in Cairo, New Cairo City, Egypt*

Stephan Schiller

*Institut für Experimentalphysik, Heinrich-Heine-Universität Düsseldorf, Universitätsstrasse 1, 40225 Düsseldorf, Germany*

Jonathan Tennyson

*Department of Physics and Astronomy, University College London, London WC1E 6BT, United Kingdom*

Stephan Schlemmer

*I. Physikalisches Institut, Universität zu Köln, Zùlpicher Strasse 77, 50937 Köln, Germany*

(Received 9 August 2007; accepted 12 September 2007; published online 18 October 2007)

The method of laser induced reaction is used to obtain high-resolution IR spectra of  $\text{H}_2\text{D}^+$  and  $\text{D}_2\text{H}^+$  in collision with  $n\text{-H}_2$  at a nominal temperature of 17 K. For this purpose three cw-laser systems have been coupled to a 22-pole ion trap apparatus, two commercial diode laser systems in the ranges of  $6100\text{--}6600\text{ cm}^{-1}$  and  $6760\text{--}7300\text{ cm}^{-1}$ , respectively, and a high-power optical parametric oscillator tunable in the range of  $2600\text{--}3200\text{ cm}^{-1}$ . In total, 27 new overtone and combination transitions have been detected for  $\text{H}_2\text{D}^+$  and  $\text{D}_2\text{H}^+$ , as well as a weak line in the  $\nu_1$  vibrational band of  $\text{H}_2\text{D}^+$  ( $2_{20}\leftarrow 1_{01}$ ) at  $3164.118\text{ cm}^{-1}$ . The line positions are compared to high accuracy *ab initio* calculations, showing small but mode-dependent differences, being largest for three vibrational quanta in the  $\nu_2$  symmetric bending of  $\text{H}_2\text{D}^+$ . Within the experimental accuracy, the relative values of the *ab initio* predicted Einstein *B* coefficients are confirmed. © 2007 American Institute of Physics. [DOI: 10.1063/1.2794331]

## I. INTRODUCTION

The smallest polyatomic molecule,  $\text{H}_3^+$ , has since long fascinated chemical theorists, spectroscopists, and astronomers due to its apparent simplicity and importance in astrochemical environments. This molecule, in which the three protons are held together in a triangle by a distributed cloud of two electrons (three center-two electron bonding), has first been observed spectroscopically in the laboratory by Oka in 1980,<sup>1</sup> and since then a wealth of laboratory studies has been conducted, including fundamental, overtone, combination, and hot bands.<sup>2</sup>

For the investigation of cold interstellar clouds, the deuterated versions of  $\text{H}_3^+$ ,  $\text{H}_2\text{D}^+$ , and  $\text{D}_2\text{H}^+$  are of even greater importance, firstly because they are known to drive deuteration processes in these environments by ion-molecule exchange reactions,<sup>3</sup> leading to a wealth of deuterated species.<sup>4</sup> Even multiply deuterated molecules have been discovered in

prestellar cores (see, for example, Refs. 5–10), suggesting the importance of  $\text{D}_3^+$  in such environments.<sup>11</sup> Secondly, the  $\text{H}_2\text{D}^+$  and  $\text{D}_2\text{H}^+$  ions possess a permanent dipole moment and can thus be detected by their rotational lines. Although the  $1_{10}\text{--}1_{11}$  line of ortho- $\text{H}_2\text{D}^+$  was detected in the laboratory in 1984,<sup>12–14</sup> it took a long search until the  $\text{H}_2\text{D}^+$  ion was observed 1999 in the interstellar medium,<sup>15</sup> and five years later also the submillimeter detection of  $\text{D}_2\text{H}^+$  was reported.<sup>16</sup> Since then, the 372 GHz line of  $\text{H}_2\text{D}^+$  has been used routinely to probe the conditions in cold clouds,<sup>17–19</sup> whereas the  $\text{D}_2\text{H}^+$  detection is the only one so far.

Owing to their fundamental importance, there is a 25 year history of laboratory infrared spectroscopy of  $\text{H}_2\text{D}^+$  and  $\text{D}_2\text{H}^+$ . The first few fundamental lines of  $\text{H}_2\text{D}^+$  were observed by Shy *et al.*,<sup>20</sup> who used a Doppler-tuned fast ion beam method but gave no specific rotational assignments. Assignments were made as part of subsequent, more comprehensive cell discharge measurements of the  $\nu_2$  and  $\nu_3$  vibrational bands by Foster *et al.*,<sup>21</sup> while the  $\nu_1$  band was measured by Amano<sup>22</sup> and Lubic and Amano.<sup>23</sup> The corresponding results for the  $\text{D}_2\text{H}^+$  molecule were reported shortly thereafter<sup>24,25</sup> by those two groups. The first detection

<sup>a)</sup>Present address: I. Physikalisches Institut, Universität zu Köln, Germany. Electronic mail: asvany@ph1.uni-koeln.de

<sup>b)</sup>Also at Institut für Experimentalphysik, Heinrich-Heine-Universität Düsseldorf, Germany.

of overtone and combination bands was reported by Fárník *et al.*,<sup>26</sup> who detected the  $2\nu_2$ ,  $2\nu_3$ , and  $\nu_2 + \nu_3$  bands of  $\text{H}_2\text{D}^+$  and  $\text{D}_2\text{H}^+$  in a cold supersonic jet. As these light molecules cannot be described very well by the Born-Oppenheimer approximation, and also due to strong Coriolis coupling in the  $\text{D}_2\text{H}^+$  ion, that study was guided by and compared to high-level *ab initio* theoretical predictions.

Computational *ab initio* procedures have been developed in recent decades to provide highly accurate level predictions for few electron systems. For diatomics such as  $\text{HD}^+$  the computations can reach an accuracy far better than  $10^{-3} \text{ cm}^{-1}$ ,<sup>27,28</sup> and experiments using sympathetically cooled ions have been carried out to test those predictions.<sup>29,30</sup> For the electronically simplest triatomic,  $\text{H}_3^+$  and its isotopologues, the predictions reach “only” near-spectroscopic accuracy of better than  $0.1 \text{ cm}^{-1}$ .<sup>26,31</sup> This accuracy is still one order of magnitude better than can be obtained for a many-electron system such as water.<sup>32</sup>

For triatomics the high accuracy *ab initio* calculation of molecular vibration-rotation spectra involves the use of variational nuclear motion calculations<sup>33</sup> and a high accuracy potential energy surface. For the  $\text{H}_3^+$  system, Cencek *et al.*<sup>34</sup> calculated a potential energy surface with an absolute accuracy of  $0.04 \text{ cm}^{-1}$ . They also computed an electronic relativistic correction for this surface, although this only has a very minor influence on the spectrum. Of more significance are corrections due to failure of the Born-Oppenheimer approximation.<sup>35–37</sup> Polyansky and Tennyson<sup>38</sup> developed a high accuracy model based on the *ab initio* calculations of Cencek *et al.*, including, in particular, a refit of their adiabatic correction, and a model of nonadiabatic effects based on the use of the effective vibrational masses obtained by Moss for the  $\text{H}_2^+$  system.<sup>39</sup> The predictive nature of this model has been tested by Fárník *et al.*<sup>26</sup> and, more recently, by Hlavenka *et al.*<sup>40</sup> for  $\text{H}_2\text{D}^+$  and  $\text{D}_2\text{H}^+$  ions, respectively. Given their greater sensitivity to corrections to the Born-Oppenheimer approximation,<sup>35,36</sup> the deuterated isotopologues provide a particularly stringent test of the theory.

For astronomical studies it is important to have accurate line positions as well as reliable transition intensities. Although such studies are based on experimental line positions (e.g., Ref. 41), they have to rely on *ab initio* predictions of the transition strength (e.g., Ref. 42). There is considerable indirect evidence that these transition strengths are indeed reliable, but the measurements by Fárník *et al.*<sup>26</sup> raised some doubts about this issue. Extensive tests on the theory<sup>43</sup> failed to identify any significant errors. Therefore, testing the reliability of the line strength predictions is one of the objectives of the present study.

This work uses the technique of laser induced reactions (LIRs) to obtain high-resolution overtone spectra of  $\text{H}_2\text{D}^+$  and  $\text{D}_2\text{H}^+$ . In contrast to the direct absorption spectroscopy methods listed above, the transitions are detected by the action of the laser light on the ion species, as, for example, an induced chemical reaction with  $n\text{-H}_2$  (see below). Several examples of the feasibility of this approach for  $\text{H}_3^+$  isotopomers have already been published.<sup>44–46</sup> This work is organized as follows. The spectroscopic aspects of LIR are summarized and an introduction is given to the low-temperature

22-pole trapping apparatus, as well as the three laser systems used in this work. In Sec. IV the measured overtone line positions are summarized for  $\text{H}_2\text{D}^+$  and  $\text{D}_2\text{H}^+$ , and also some new data for the  $\nu_1$  transition of  $\text{H}_2\text{D}^+$  are shown. These experimental results are then compared to the theoretical *ab initio* predictions, line positions, as well as Einstein *B* coefficients. Furthermore, the measured Doppler widths and the influence of Coriolis coupling and Fermi resonances are discussed. The present work provides basic spectroscopic tools to probe the rotational level population of the presented ions, which will be the topic of a follow-up publication.<sup>47</sup>

## II. EXPERIMENTAL ASPECTS

### A. LIRs of $\text{H}_2\text{D}^+$ and $\text{D}_2\text{H}^+$

LIR belongs to the family of “action spectroscopy” methods where the influence of the laser light on the mass-selected ions investigated is monitored by detecting changes induced to the trapped ion cloud composition. Detection is usually achieved very efficiently using an ion counter. In the special case of LIR, changes of the rate of an endothermic ion-molecule reaction serve to detect the excitation of the parent ionic species. This offers not only the possibility of doing very high sensitivity spectroscopy on transient ions (a number of only 1000 ions per trapping period is sufficient), but LIR can also yield, for example, information on state-selected reaction rate coefficients, inelastic collision rate coefficients, lifetimes of excited states, or the population of rotational states.

Recent examples of this method include the IR spectroscopy of the highly fluxional  $\text{CH}_5^+$  molecule,<sup>48–50</sup> the laser induced charge transfer in the system  $\text{N}_2^+ + \text{Ar}$ ,<sup>51</sup> and the spectroscopy of the infrared active stretching and bending motions<sup>52–54</sup> of  $\text{C}_2\text{H}_2^+$  via the abstraction reaction  $\text{C}_2\text{H}_2^+ + \text{H}_2 \rightarrow \text{C}_2\text{H}_3^+ + \text{H}$ . In this latter scheme, the endothermicity of about  $50 \text{ meV}$  ( $=403 \text{ cm}^{-1}$ ) is overcome by the rovibrational energy of the laser excited molecule. More recently, also the overtone spectroscopy and the corresponding population and temperature diagnostic have been demonstrated for  $\text{H}_3^+$  in reaction with Ar atoms at a nominal temperature of  $50 \text{ K}$ ,<sup>44</sup> and a similar work has been carried out for  $\text{D}_2\text{H}^+$ .<sup>45</sup>

Here the lowest rotational states of  $\text{H}_2\text{D}^+$  and  $\text{D}_2\text{H}^+$  are probed by exciting their overtone and combination transitions and also using the  $\nu_1$  band for  $\text{H}_2\text{D}^+$ . While the fundamental  $\nu_1$  band is well studied,<sup>22,23,31,55</sup> and the states of  $\text{H}_3^+$  have been explored up to high levels of excitation,<sup>2</sup> the experimental search for overtone/combination rovibrational transitions of  $\text{H}_2\text{D}^+$  and  $\text{D}_2\text{H}^+$  has only recently started.<sup>26</sup> In the following, the basic processes of interest for the spectroscopic aspects of LIR are summarized with help of Fig. 1 for  $\text{H}_2\text{D}^+$ , but are similar for  $\text{D}_2\text{H}^+$ . For LIR of  $\text{H}_2\text{D}^+$ , the exchange reaction



is used. This reaction is endothermic by about  $232 \text{ K}$  for  $\text{H}_2\text{D}^+$  in the lowest rotational state  $0_{00}$  and about  $146 \text{ K}$  for the  $1_{11}$  orthostate (see the dashed line in the figure), and its overall rate coefficient  $k$  has been measured to be small at

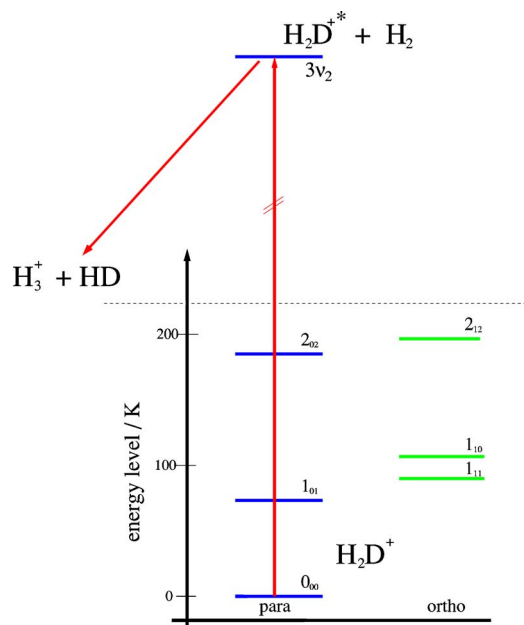
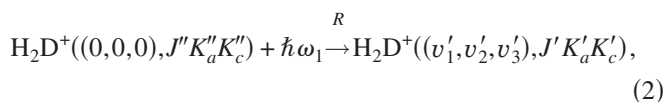
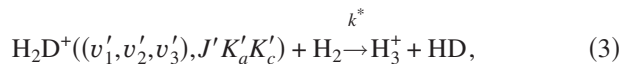


FIG. 1. (Color online) LIR spectroscopy exploits the change in speed of an ion-molecule reaction to detect the excitation of the ion involved. For the spectroscopy of H<sub>2</sub>D<sup>+</sup> the collision with H<sub>2</sub>, reaction (1), leading to the ionic product H<sub>3</sub><sup>+</sup> is used. This reaction is endothermic by 232 K as indicated by the dashed line. As only the lowest rotational levels of H<sub>2</sub>D<sup>+</sup> are populated at the low temperature of the experiment, the reaction is initially slow. Its speed can be substantially increased by exciting the ion prior to collision with the H<sub>2</sub> molecule.

low temperatures. Adams and Smith<sup>56</sup> measured a value of  $2.9 \times 10^{-10} \text{ cm}^3 \text{ s}^{-1}$  for the reaction with *n*-H<sub>2</sub> at 80 K, and Gerlich *et al.*<sup>3</sup> obtained a value of  $4.9 \times 10^{-11} \text{ cm}^3 \text{ s}^{-1}$  at a nominal temperature of 10 K. The slowness of this reaction at low temperatures renders LIR spectroscopy feasible by first exciting the ion (with rate *R*), starting from the ground vibrational level (0,0,0),



into a particular rovibrational level. Here,  $(v'_1, v'_2, v'_3)$  indicate the quanta in the three vibrational modes of H<sub>2</sub>D<sup>+</sup>. Once excited, the H<sub>2</sub>D<sup>+</sup> ion can react much faster with a H<sub>2</sub> target molecule (with rate coefficient  $k^* > k$ ),



leading to an enhancement in the counts of H<sub>3</sub><sup>+</sup> product ions. Thus, by counting these product ions as a function of the laser wavelength, a LIR spectrum is obtained. For maximal signal counts in the LIR experiment, the collision rate with the neutral reaction partner H<sub>2</sub> should be similar to the decay rate *A* of the excited H<sub>2</sub>D<sup>+</sup> ion,

$$k_c[\text{H}_2] \geq A. \quad (4)$$

In the above relation, [H<sub>2</sub>] is the number density of the neutral reaction partner (given in cm<sup>-3</sup>). The rate coefficient *k<sub>c</sub>* for the collision of H<sub>2</sub>D<sup>+</sup> with H<sub>2</sub> can be assumed to be the Langevin rate coefficient *k<sub>L</sub>*, which is calculated to be  $k_c \approx k_L = 1.80 \times 10^{-9} \text{ cm}^3 \text{ s}^{-1}$  ( $1.74 \times 10^{-9} \text{ cm}^3 \text{ s}^{-1}$  for D<sub>2</sub>H<sup>+</sup>).

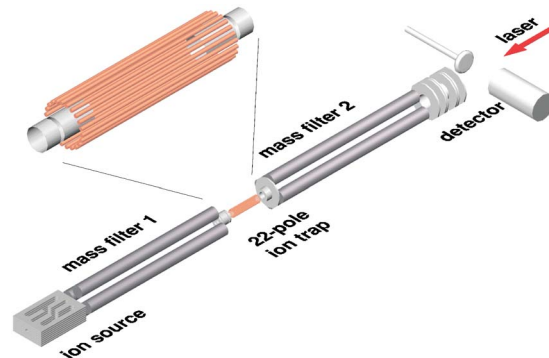


FIG. 2. (Color online) Schematic setup of the trapping apparatus as used for laser induced reactions (LIRs). The ions are generated and collected in the storage ion source, mass selected in the quadrupole mass filter 1, and then stored in the 22-pole ion trap. This trap, consisting of 22 rf electrodes forming a cylindrical structure (see inset), is mounted on a closed cycle helium refrigerator. On entrance the ions are cooled down to the ambient cryogenic temperature by a short intense pulse of cold He atoms. During the storage period of typically 1 s, the ions are subject to reactant gas molecules and tunable laser light (coming from the right through the axially transparent setup). The result of this interaction is detected by extracting the stored ion cloud into mass filter 2 and counting the number of product ions in the detector. By repeating this process while scanning the IR laser, an IR action spectrum of the stored parent ions is recorded.

## B. 22-pole ion trap apparatus

The experimental procedure is described using the setup shown in Fig. 2. The central part of this apparatus is a 22-pole ion trap which has been described in detail by Gerlich.<sup>57,58</sup> The H<sub>2</sub>D<sup>+</sup> parent ions are generated in the storage ion source by ionization of hydrogen gas containing D<sub>2</sub> admixtures of several percent (5%–15%). All H<sub>3</sub><sup>+</sup> isotopologues are produced by reactions of the type H<sub>2</sub><sup>+</sup>+H<sub>2</sub>→H<sub>3</sub><sup>+</sup>+H and subsequent exchange reactions with the neutral gas. The ionization energy is kept at about 22 eV to allow for an efficient production of the parent ions. By trapping the ions in the source, the pressure of the precursor gas mixture can be kept below 10<sup>-5</sup> mbar and the produced cations are cooled to the source temperature of 350 K by collisions. Low source pressures are essential for this type of experiment because gases leaking into the trap region would disturb the chemistry there.

The first mass filter is operated in a mode to admit only ions with masses greater than 3 u [i.e., H<sub>2</sub>D<sup>+</sup>, (D<sub>2</sub>)<sup>+</sup>, D<sub>2</sub>H<sup>+</sup>, and D<sub>3</sub><sup>+</sup>] into the 22-pole ion trap. This allows spectroscopy to be performed on all of the admitted ions simultaneously. D<sub>2</sub><sup>+</sup> impurities, with mass of 4 u, react very fast to form H<sub>3</sub><sup>+</sup> isotopologues in the hydrogen environment of the trap. Usually the average number of H<sub>2</sub>D<sup>+</sup> ions injected into the 22-pole trap is about 700. The trap is driven by a rf power of 17 MHz frequency and about V<sub>0</sub>=15 V amplitude. In this field, the ion cloud is typically stored for 1 s embedded in a cold *n*-H<sub>2</sub> gas environment and exposed to the tunable IR light. The number density of H<sub>2</sub> (commercial grade 6.0) is about  $5 \times 10^{10} \text{ cm}^{-3}$  to offer enough collision possibilities with the excited H<sub>2</sub>D<sup>+</sup> within their lifetime. The trap temperature is kept at its lowest possible value. The closed cycle helium refrigerator to which the trap setup is mounted has a nominal temperature of 10 K at its tip. A temperature of



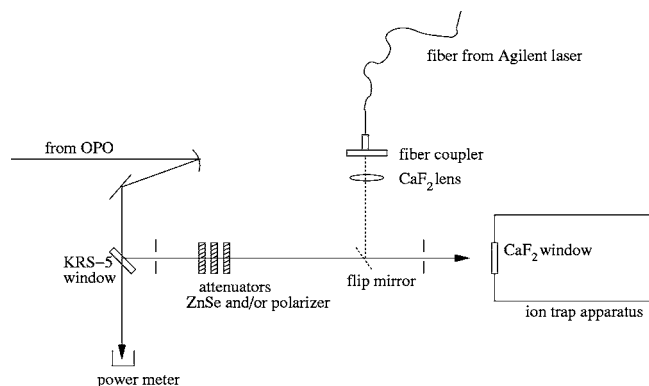


FIG. 3. Setup of optical components on the laser table attached to the trapping machine. A flip mirror mount allowed to change between the laser light of the commercial Agilent diode lasers and the homemade OPO system. As the OPO power is quite high (up to 50 mW), several attenuators (ZnSe windows, a KRS-5 window, and a polarizer) have been used to weaken the laser power to levels below 1 mW. By means of the KRS-5 window the beam is split and the relative power is measured.

$17 \pm 1$  K is measured with a silicon diode sensor at the trap housing on the opposite side of the cold head tip.

After the storage period, the content of the trap is extracted, mass selected in the second quadrupole mass filter, and the ionic reaction product  $\text{H}_3^+$  is counted in the Daly-type ion detector. The experiment is run in a shot-by-shot mode, i.e., the laser is tuned to the next frequency step and the process of *trapping/irradiation/reaction/detection* is repeated again, by which a spectrum is recorded. The shots can be repeated several times at the same frequency to improve the S/N ratio.

### C. Laser systems

Two different laser systems have been used for the experiment. The first set of lasers was Agilent 8164A diode laser controllers with diode laser modules 81642A and 81480A operating in the frequency ranges of  $6097\text{--}6622\text{ cm}^{-1}$  (1510–1640 nm) and  $6757\text{--}7299\text{ cm}^{-1}$  (1370–1480 nm), respectively. The output power was varying over the frequency ranges with a maximum of about 5.5 mW. The diodes could be tuned and computer controlled with a precision of 0.0001 nm (i.e., about  $0.0005\text{ cm}^{-1} = 15\text{ MHz}$ ). The intrinsic linewidth of the lasers is specified to about 100 kHz, but exhibits broadening to several megahertz due to frequency jitter. The calibrations of the diode lasers were first checked with two Burleigh wavemeters of the type WA-1500. As these calibrations turned out to be insufficient, the Agilent lasers have been compared to  $\text{H}_2\text{O}$  and  $\text{CO}_2$  absorption lines which are tabulated with a precision better than  $0.001\text{ cm}^{-1}$  in the HITRAN database.<sup>59</sup> In total, the laser line positions measured in this work are accurate within  $0.002\text{ cm}^{-1}$ . The laser light was sent via an optic fiber to the laser table of the trapping machine, where it was steered via a collimator, a  $\text{CaF}_2$  lens, a flip mirror, and a differentially pumped vacuum window<sup>60</sup> into the 22-pole ion trap, see Fig. 3. No nitrogen flushing was necessary on the short path of the laser table, as the water absorptions in the investigated frequency regions are quite weak.

The second laser system used in the experiments was a optical parametric oscillator (OPO) operating in the  $3\text{ }\mu\text{m}$  region. This OPO is a homemade high-power tunable cw system in which photons from a pump yttrium aluminum garnet laser at about  $\omega_p = 9394\text{ cm}^{-1}$  (1064 nm) are split in a periodically poled lithium niobate crystal into signal and idler photons according to  $\omega_s + \omega_i = \omega_p$ .<sup>61</sup> The idler beam of the OPO is tunable in the range of  $2600\text{--}3200\text{ cm}^{-1}$  and can reach a maximum power of 50 mW. For high precision determination of the lines, two Burleigh wavemeters have been used to measure simultaneously the frequencies of the pump and signal beam, giving an accuracy of about  $0.003\text{ cm}^{-1}$ . Where lower accuracy was required, only one wavemeter was used to measure the signal beam, assuming the pump frequency did not vary appreciably. As shown in Fig. 3, a KRS-5 window was used as a beam splitter to send about 13% of the laser power to the 22-pole trapping apparatus and the remaining 87% into a power meter. The idler beam could be further attenuated to sub-mW power levels by additional beam inserts.

The OPO has a short-term intrinsic linewidth of some kilohertz and a stability of several megahertz during the trapping time of 1 s,<sup>61</sup> which is much smaller than the Doppler width  $\sigma_D = 70\text{ MHz}$  of the corresponding transitions (see following sections). Problems arose initially due to mode hops of the OPO system, rendering the spectroscopy difficult. This problem was solved by the data acquisition software, which rejected any data points when the wavemeters indicated frequency jumps during trapping time.

### III. AB INITIO PREDICTIONS

The line positions and corresponding wave functions were calculated using the model of Polyansky and Tennyson.<sup>38</sup> Nuclear motion calculations were performed in Jacobi coordinates with the DVR3D program suite<sup>62</sup> and used basis sets optimized for previous studies.<sup>43</sup> Einstein *A* coefficients were calculated using the *ab initio* dipole surfaces of Röhse *et al.*<sup>37</sup>

Variational nuclear motion calculations only use the rigorous quantum numbers of the system, for  $\text{H}_2\text{D}^+$  and  $\text{D}_2\text{H}^+$  these are the total rotational angular momentum  $J$ , parity  $p$ , and the nuclear spin state (ortho- or para-). Here approximate vibrational ( $v_1, v_2, v_3$ ) and rotational ( $K_a, K_c$ ) quantum numbers were assigned by hand based on a simple analysis of the energy patterns in the two systems. This procedure is not general and can be hard to apply for  $\text{H}_2\text{D}^+$  and  $\text{D}_2\text{H}^+$  as they show strong Coriolis effects which leads to strong mixing between vibrational states. However, the present experiments were performed at very low temperatures, meaning that only states starting from the  $J=0, 1$ , and 2 states of the vibrational ground states needed to be considered. For these low- $J$  states the sparsity of levels means that the assignments could be made unambiguously. The systematic errors shown by different bands which are discussed below (Sec. IV B) act as confirmation that this assignment procedure is indeed correct.

## IV. RESULTS AND DISCUSSION

### A. Detection of H<sub>2</sub>D<sup>+</sup> and D<sub>2</sub>H<sup>+</sup> transitions

#### 1. Second overtone and combination bands

The H<sub>2</sub>D<sup>+</sup> transitions were measured by applying LIR to reaction (1), while the laser excited D<sub>2</sub>H<sup>+</sup> ions were detected by counting the same product ion (H<sub>3</sub><sup>+</sup>) of the similar reaction



in which the excited D<sub>2</sub>H<sup>+</sup> ion transfers a proton to the hydrogen molecule. These LIR schemes have proven to work well in a previous study in which the fundamental bands  $\nu_2$  and  $\nu_3$  of H<sub>2</sub>D<sup>+</sup> and D<sub>2</sub>H<sup>+</sup> have been excited by the powerful free-electron laser for infrared experiments (FELIX).<sup>46</sup> That the respective ions are indeed responsible for the increase of H<sub>3</sub><sup>+</sup> counts in their LIR spectra has been checked by mass spectrometric means in selected cases. For the line detections the density of the H<sub>2</sub> reactant was about  $4 \times 10^{10} \text{ cm}^{-3}$ , the trapping time was between 1 and 2 s, and the laser power varying from 1.5 to 5.5 mW. The trap was kept at its lowest nominal temperature of about 17 K. Therefore, only transitions starting from the lowest rotational levels of H<sub>2</sub>D<sup>+</sup> (see Fig. 1) and D<sub>2</sub>H<sup>+</sup> could be expected. The detections were guided by high accuracy *ab initio* calculations, from which the strongest transitions falling into the wavelength range of the lasers have been selected for the search. As an example, the strongest transitions detected for H<sub>2</sub>D<sup>+</sup> [(0,2,1) 1<sub>11</sub> ← 0<sub>00</sub>] and one weak transition for D<sub>2</sub>H<sup>+</sup> [(1,1,1) 0<sub>00</sub> ← 1<sub>01</sub>] are shown in Fig. 4. To increase the S/N ratio, the scan was repeated ten times for the strong H<sub>2</sub>D<sup>+</sup> signal, while averaging over 30 scans was necessary for the D<sub>2</sub>H<sup>+</sup> peak shown. The background of H<sub>3</sub><sup>+</sup> ions has been subtracted in both cases. The good S/N ratio for most of the measured peaks allowed their relative positions to be determined to better than  $10^{-3} \text{ cm}^{-1}$ , but the total accuracy was limited by the calibration of the diode lasers with an accuracy better than  $2 \times 10^{-3} \text{ cm}^{-1}$  (see Sec. II). A total of 20 H<sub>2</sub>D<sup>+</sup> and 7 D<sub>2</sub>H<sup>+</sup> lines have been detected which are summarized in Tables I and II together with their assignments. Also given in the tables are the *ab initio* computed transition wave numbers and the Einstein  $A_{ul}$  coefficients ( $u$ =upper,  $l$ =lower).<sup>63</sup> The total decay constants  $A_{\text{tot}} = \sum_l A_{ul}$  of the upper states have also been calculated from a comprehensive list of such transitions. While  $A_{ul}$  characterizes the decay of the excited ion back into the specific state where it came from,  $A_{\text{tot}}$  gives the overall decay rate of the upper state. More interesting in the case of LIR is the effective decay constant  $A_{\text{eff}}$ , specifying the time the excited ion needs to cascade back into the ground vibrational state,

$$A_{ul} < A_{\text{eff}} < A_{\text{tot}}. \quad (6)$$

For the transitions summarized in Tables I and II, the effective decay constants  $A_{\text{eff}}$  of the corresponding upper states have been calculated by solving a complete rate equation system including all relevant rovibrational energy levels. This procedure is similar to that described by Kreckel *et al.*<sup>64</sup> By solving the rate equations, an effective decay constant  $A_{\text{eff}}$  between 25 and 35 s<sup>-1</sup> has been determined for various upper levels of both species. This quantity is an im-

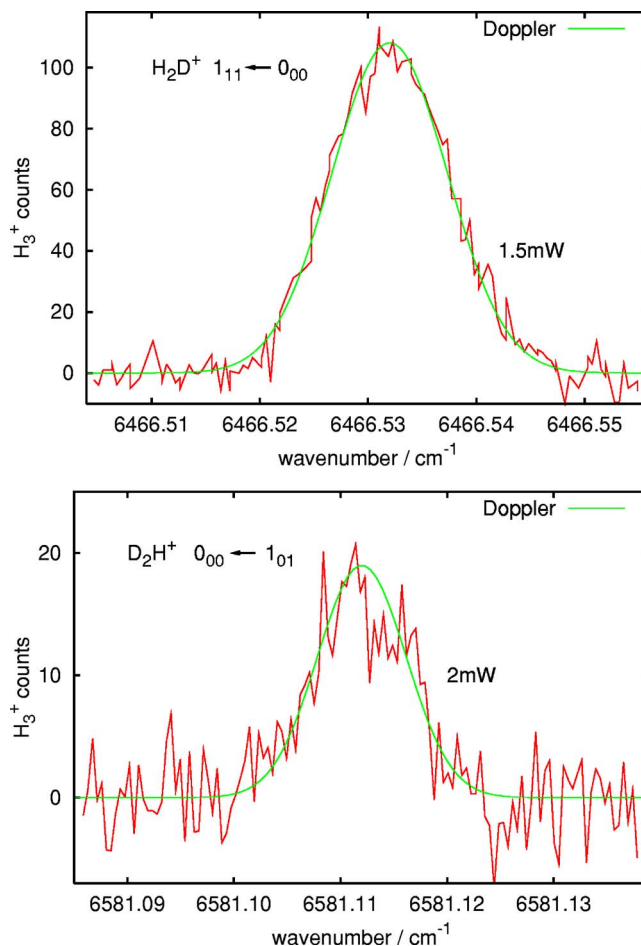


FIG. 4. (Color online) Two representative combination band transitions measured with the Agilent diode laser, the strongest peak for H<sub>2</sub>D<sup>+</sup> at  $6466.532 \text{ cm}^{-1}$  [(0,2,1) 1<sub>11</sub> ← 0<sub>00</sub>], and one of the weakest peaks measured for D<sub>2</sub>H<sup>+</sup> at  $6581.112 \text{ cm}^{-1}$  [(1,1,1) 0<sub>00</sub> ← 1<sub>01</sub>]. The storage times were 1.5 and 2 s, respectively, and the laser power is indicated in the figures. The constant H<sub>3</sub><sup>+</sup> background count of several hundred ions per trap filling has been subtracted. The H<sub>2</sub>D<sup>+</sup> peak shape follows a Doppler profile, yielding a fitted kinetic temperature of  $27 \pm 2 \text{ K}$ .

portant parameter in LIR as to guarantee that the excited ions meet a H<sub>2</sub> reaction partner before fluorescing back to the vibrational ground state, see relation (4). For example, a H<sub>2</sub> number density of at least  $4 \times 10^{10} \text{ cm}^{-3}$  and a collision rate coefficient  $k_c = 1.8 \times 10^{-9} \text{ cm}^3 \text{ s}^{-1}$  for H<sub>2</sub>D<sup>+</sup>+H<sub>2</sub> yield a collision rate of more than  $72 \text{ s}^{-1}$ , which is high enough to compete with the effective rate  $A_{\text{eff}}$  given above.

For H<sub>2</sub>D<sup>+</sup>, the measured transitions fall into three well separated vibrational overtones or combination bands, each of them containing at least two quanta in the  $\nu_2$  bending mode. It is interesting to note that the different character of these bands is mirrored in the decay constant  $A_{\text{tot}}$  (see the corresponding column in Table I), as well as in the difference to the *ab initio* computed transition wave numbers (Sec. IV B). The same is true for D<sub>2</sub>H<sup>+</sup>. The transition at  $6581.112 \text{ cm}^{-1}$ , the only one measured for the (1,1,1) band, has an upper level with a remarkably short lifetime, and it also exhibits a different offset to the calculated frequency values (see Fig. 6 lower) than the other D<sub>2</sub>H<sup>+</sup> transitions. The rest of the D<sub>2</sub>H<sup>+</sup> transitions belong to the (1,2,0) and (1,0,2) bands which are mixed by Fermi resonances (see Sec. IV C). Accordingly, their lifetimes  $A_{\text{tot}}$  show similar values.

TABLE I. Second overtone and combination transitions of  $\text{H}_2\text{D}^+$  (in  $\text{cm}^{-1}$ ) detected with the diode laser systems. The overall experimental accuracy is about  $0.002 \text{ cm}^{-1}$ . The *ab initio* transition wave numbers and Einstein  $A_{ul}$  coefficients (in  $\text{s}^{-1}$ ) are taken from a line list (Ref. 63) which was calculated according to the procedures described in Ref. 38. From this list, the lifetimes of the upper states  $\tau=1/A_{\text{tot}}$  were determined. Also, the Einstein  $B_{lu}$  coefficients have been calculated from the  $A_{ul}$  according to Eq. (8) and normalized to the strongest transition at  $6466.532 \text{ cm}^{-1}$ .

	Transition	This work	Calc.	$A_{ul}$	$A_{\text{tot}}$	$g_u/g_l$	$B_{lu}$
(0,3,0)	$0_{00} \leftarrow 1_{01}$	6241.966	6242.121	7.08	154.7	1/3	0.21
(0,3,0)	$1_{11} \leftarrow 1_{10}$	6270.392	6270.544	2.13	156.9	3/3	0.19
(0,3,0)	$1_{10} \leftarrow 1_{11}$	6303.784	6303.941	3.36	154.5	3/3	0.29
(0,3,0)	$1_{01} \leftarrow 0_{00}$	6330.973	6331.127	1.21	158.7	3/1	0.31
(0,2,1)	$0_{00} \leftarrow 1_{11}$	6340.688	6340.778	9.36	268.1	1/3	0.27
(0,2,1)	$1_{01} \leftarrow 1_{10}$	6369.460	6369.557	6.04	267.4	3/3	0.51
(0,2,1)	$1_{10} \leftarrow 1_{01}$	6433.742	6433.833	4.64	270.3	3/3	0.38
(0,2,1)	$2_{02} \leftarrow 1_{11}$	6459.036	6459.133	2.47	269.8	5/3	0.34
(0,2,1)	$1_{11} \leftarrow 0_{00}$	6466.532	6466.635	4.10	271.6	3/1	1
(0,2,1)	$3_{03} \leftarrow 2_{12}$	6483.576	6483.681	3.86	282.7	7/5	0.44
(0,2,1)	$2_{12} \leftarrow 1_{01}$	6491.349	6491.451	4.49	266.8	5/3	0.60
(0,2,1)	$2_{21} \leftarrow 1_{10}$	6573.837	6573.925	3.64	280.7	5/3	0.47
(0,2,1)	$2_{20} \leftarrow 1_{11}$	6589.412	6589.505	2.49	280.9	5/3	0.32
(1,2,0)	$0_{00} \leftarrow 1_{01}$	6945.877	6945.868	10.25	105.2	1/3	0.22
(1,2,0)	$1_{11} \leftarrow 1_{10}$	6974.252	6974.253	5.54	117.0	3/3	0.36
(1,2,0)	$1_{10} \leftarrow 1_{11}$	7004.803	7004.794	5.10	105.5	3/3	0.33
(1,2,0)	$1_{01} \leftarrow 0_{00}$	7039.362	7039.366	3.72	121.4	3/1	0.70
(1,2,0)	$2_{12} \leftarrow 1_{11}$	7066.839	7066.878	3.60	191.0	5/3	0.37
(1,2,0)	$2_{02} \leftarrow 1_{01}$	7077.529	7077.560	4.05	170.9	5/3	0.42
(1,2,0)	$2_{11} \leftarrow 1_{10}$	7105.518	7105.505	3.38	129.9	5/3	0.35

## 2. $\nu_1$ vibrational band

In a further series of experiments, the  $3 \mu\text{m}$  cw-OPO laser system has been used for the spectroscopy of the  $\nu_1$  band of  $\text{H}_2\text{D}^+$  and to evaluate the feasibility of probing the low-temperature rotational population. This band was detected 25 years ago by Amano and Watson,<sup>22,23</sup> and later partly reassigned by Kozin *et al.*<sup>55</sup> Table III lists the five lines measured with the OPO laser and compares them to previous experimental and calculated values. The transitions from low rotational states presented here agree well with the results from Amano and Watson,<sup>22</sup> while the calculated values from Ramanlal and Tennyson<sup>31</sup> seem to be systematically higher than the experimental values by about  $0.02 \text{ cm}^{-1}$  (see next subsection for a general comparison).

The fundamental band  $\nu_1$  of  $\text{H}_2\text{D}^+$  is much stronger than the overtone and combination bands by a factor of about 50.

This can be estimated by inserting some values of  $A_{ul}$  from Tables I and II in relation (8). Additionally, the Doppler width of a transition reduces as the frequency of a transition is lowered ( $\sigma_D \sim \nu_0$ ). Therefore, only very low power was needed for the  $\nu_1$  band and the OPO power was therefore attenuated by several filters (see Fig. 3). For example, with an Einstein coefficient  $B_{lu}=1.3 \times 10^{17} \text{ m}^3/\text{J s}^2$  for the  $1_{01} \leftarrow 0_{00}$  transition at  $3038.182 \text{ cm}^{-1}$ , a laser power of  $P=0.1 \text{ mW}$  is sufficient to excite the cold ions ( $27 \text{ K}$ ) with a rate  $R \approx 4.9 \text{ s}^{-1}$ . The full power capabilities of the OPO system could be demonstrated by a hitherto undetected line which was predicted by Ramanlal and Tennyson<sup>31</sup> at the position of  $3164.149 \text{ cm}^{-1}$  with a very small Einstein  $A_{ul}$  coefficient of only  $1.598 \text{ s}^{-1}$  (Table III). For the measurement of this line, all attenuators have been taken out of the beam line (Fig. 3) and a full idler power of about  $24 \text{ mW}$  at the corre-

TABLE II. Second overtone and combination transitions of  $\text{D}_2\text{H}^+$ , for explanations see Table I. For comparison, also two transitions measured by cw-CRDS (Refs. 40 and 45) are listed. The values of the Einstein  $A_{ul}$  coefficients given here are about three times smaller than those for  $\text{H}_2\text{D}^+$ , making the detection of  $\text{D}_2\text{H}^+$  somewhat more difficult. The Einstein  $B_{lu}$  coefficients are given relative to the transition at  $6536.319 \text{ cm}^{-1}$ .

	Transition	This work	Ref. 40	Calc.	$A_{ul}$	$A_{\text{tot}}$	$g_u/g_l$	$B_{lu}$
(1,2,0)	$1_{01} \leftarrow 1_{10}$	6466.936		6466.916	2.41	160.9	3/3	0.49
(1,2,0)	$1_{11} \leftarrow 0_{00}$	6482.033		6482.011	0.53	149.6	3/1	0.32
(1,2,0)	$2_{20} \leftarrow 1_{11}$	6518.523		6518.511	1.88	151.1	5/3	0.62
(1,0,2)	$1_{10} \leftarrow 1_{01}$	6524.010		6523.987	1.27	165.2	3/3	0.25
(1,2,0)	$2_{12} \leftarrow 1_{01}$	6535.953	6535.950	6535.943	2.28	157.4	5/3	0.75
(1,0,2)	$1_{11} \leftarrow 0_{00}$	6536.319	6536.319	6536.301	1.68	171.1	3/1	1
(1,1,1)	$0_{00} \leftarrow 1_{01}$	6581.112		6581.141	4.35	255.1	1/3	0.28

TABLE III. Transitions (in cm<sup>-1</sup>) of the (1,0,0) band of H<sub>2</sub>D<sup>+</sup> detected with the OPO system, for further explanations see Table I. The accuracy of the OPO measurements using two wavemeters is 0.003 cm<sup>-1</sup> and thus similar to the accuracy of Amano and Waston (Ref. 22) and Amano (Ref. 23). The *ab initio* calculated values (Ref. 63) were published by Ramanlal and Tennyson (Ref. 31).

Transition	This work	Ref. 22	Calc.	$A_{ul}$	$A_{tot}$	$g_u/g_l$	$B_{lu}$
0 <sub>00</sub> ← 1 <sub>01</sub>	2946.805	2946.802	2946.826	53.167	53.4	1/3	0.318
1 <sub>10</sub> ← 1 <sub>11</sub>	3003.279	3003.276	3003.304	27.509	53.4	3/3	0.466
1 <sub>01</sub> ← 0 <sub>00</sub>	3038.182	3038.177	3038.198	20.353	53.9	3/1	1
2 <sub>12</sub> ← 1 <sub>11</sub>	3068.850	3068.845	3068.860	20.088	54.3	5/3	0.532
2 <sub>02</sub> ← 1 <sub>01</sub>		3077.611	3077.626	24.757	54.8	5/3	0.650
2 <sub>11</sub> ← 1 <sub>10</sub>		3094.671	3094.690	19.302	54.6	5/3	0.64
2 <sub>20</sub> ← 1 <sub>01</sub>	3164.118		3164.149	1.5976	53.1	5/3	0.04

sponding laser frequency was directed to the ion trap. The 2<sub>20</sub> ← 1<sub>01</sub> line measured with the cw-OPO is depicted in Fig. 5, and its line position is determined to be at 3164.118 cm<sup>-1</sup>. In the figure, the H<sub>3</sub><sup>+</sup> signal counts were background corrected (about 500 background ions) and normalized to the measured laser power. The Doppler width of this peak and all other transitions of the  $\nu_1$  band have measured values of about  $\sigma_D=75$  MHz. Subtracting the slight broadenings caused by the two wavemeters and the jitter of the OPO on the time scale of 1 s leads to similar kinetic temperatures of the H<sub>2</sub>D<sup>+</sup> ion as measured with the Agilent diode lasers at higher wave numbers (see Sec. IV D).

## B. Comparison of experimental to computed line positions

The experimental line positions compiled in Tables I–III are compared to the high accuracy *ab initio* calculations in Fig. 6 together with other experimental work on fundamentals<sup>21,22,24,25</sup> and overtone/combination bands<sup>26</sup> performed over the last 25 years. The previous experimental work on the fundamentals was carried out in discharge tubes and therefore the elevated ion temperatures allowed a wealth of lines to be detected, from which only the transitions from the four lowest rotational levels are depicted in Fig. 6 for simplicity.

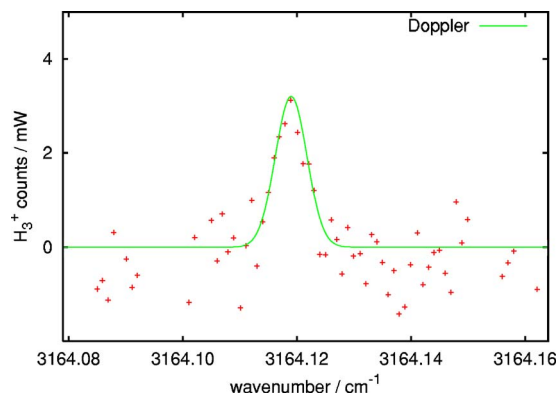


FIG. 5. (Color online) H<sub>2</sub>D<sup>+</sup> transition in the  $\nu_1$  vibrational band (2<sub>20</sub> ← 1<sub>01</sub>) at 3164.118 cm<sup>-1</sup> as measured with the OPO system. It was predicted by Ramanlal and Tennyson (Ref. 31) to be at 3164.149 cm<sup>-1</sup>. The detection of this weak transition was possible by exploiting the high cw power of 24 mW at this frequency. The Doppler width of about  $\sigma_D=75$  MHz confirms the low kinetic temperatures of the ions.

As can be seen, the deviations between experiment and theory show a clear dependence on the specific vibrational band; a systematic dependence of the deviations on rotational quantum numbers could not be observed. Heavier molecules violate less the Born-Oppenheimer approximation,

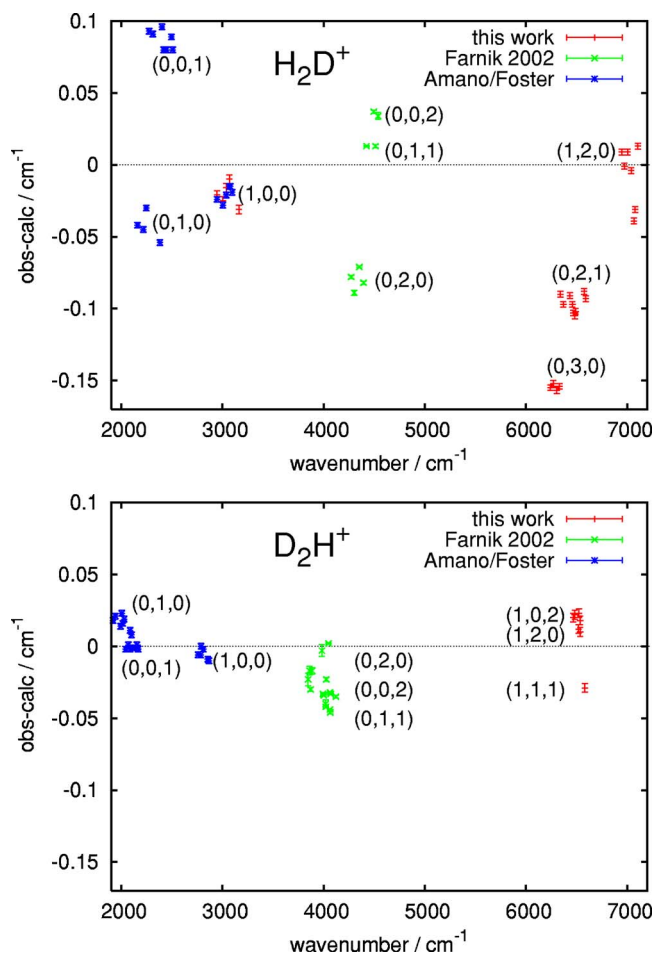


FIG. 6. (Color online) Comparison of experimentally determined fundamental, overtone, and combination transitions of H<sub>2</sub>D<sup>+</sup> and D<sub>2</sub>H<sup>+</sup> to high accuracy *ab initio* calculations (Refs. 31 and 38). The measured transitions comprise the fundamentals (Refs. 21, 22, 24, and 25), some first [Fárník *et al.* (Ref. 26)] and some second overtone and combination transitions (this work). Experimental accuracies are marked by error bars. Although deviations from the Born-Oppenheimer approximation are explicitly included in the *ab initio* predictions, the deviations for H<sub>2</sub>D<sup>+</sup> are visibly greater than for D<sub>2</sub>H<sup>+</sup>. For H<sub>2</sub>D<sup>+</sup>, the deviations depend on the specific vibrational band ( $\nu_1, \nu_2, \nu_3$ ) and are greatest when there are three quanta in the bending mode  $\nu_2$ .



and indeed the differences between experiment and calculations are visibly smaller for the heavier  $D_2H^+$  molecule, even though non-Born-Oppenheimer terms are included explicitly in the *ab initio* predictions. The greatest deviations between calculation and measurements are seen for the bending mode  $\nu_2$  in  $H_2D^+$ , and with three quanta in this mode the vibrational band (0,3,0) reaches a maximum deviation of  $0.15\text{ cm}^{-1}$ . It has already been observed with cavity ringdown spectroscopy (CRDS) experiments,<sup>40</sup> that the *ab initio* model developed by Polyansky and Tennyson<sup>38</sup> is better in predicting stretching frequencies ( $\nu_1$  and  $\nu_3$ ) than frequencies for the  $\nu_2$  bending motion. Furthermore, for  $H_2D^+$  the  $\nu_2$  and  $\nu_3$  and the  $2\nu_2$  and  $2\nu_3$  states show an approximately equal and opposite error in the *ab initio* predictions. This is precisely the behavior expected from a less than complete treatment of Born-Oppenheimer failure.<sup>36</sup> This effect is less marked for  $D_2H^+$  for which, in any case, the errors and Born-Oppenheimer correction terms are smaller.

In the (1,2,0) band of  $H_2D^+$  there are two transitions at  $7066.839$  and  $7077.529\text{ cm}^{-1}$  which fall outside the band group in Fig. 6. These two transitions also show a higher  $A_{\text{tot}}$  in Table I. The reason for this differing behavior is most probably that these levels are subject to Coriolis coupling (see next section) with rotational sublevels of the band (0,0,3) (which is not measured in this work). The magnitude of the *C*-axis Coriolis coupling is proportional to the quantum number  $K_c$ .<sup>26</sup> The strong deviation only for these two transitions thus relies on upper levels with  $K_c=2$  and apparently on near-accidental degeneracies.

### C. Coriolis coupling and Fermi resonances

The spectroscopic assignments of the fundamental  $\nu_2$  and  $\nu_3$  vibrations of  $H_2D^+$  and  $D_2H^+$  were already hampered by the fact that these modes are coupled by the Coriolis interaction.<sup>21,25</sup> Both  $H_2D^+$  and  $D_2H^+$  belong to the  $C_{2v}$  symmetry group and the bending mode  $\nu_2$  and the antisymmetric stretch  $\nu_3$  (with symmetries  $A_1$  and  $B_2$ , respectively) can couple by a rotational motion with symmetry  $B_2$ , which is, in fact, the rotation about the out-of-plane *C* axis. Fárnik *et al.*<sup>26</sup> also observed strong Coriolis coupling between the combination band (0,1,1) (symmetry  $B_2$ ) and overtone (0,0,2) (symmetry  $A_1$ ) for both molecules. For  $D_2H^+$ , the small difference in band origins ( $\Delta\nu_0 \approx 18\text{ cm}^{-1}$ ) leads to large shifts and, in fact, inverts the zeroth-order asymmetric top level structure in several instances.

Similar resonance effects can be expected for the second overtone and combination bands of  $H_2D^+$  and  $D_2H^+$  which are only qualitatively discussed here. From the detected  $H_2D^+$  bands, (0,2,1) (symmetry  $B_2$ ) can couple to the other two bands (0,3,0) and (1,2,0) (both  $A_1$ ) by *C*-axis Coriolis coupling, although the difference in band origins suggests that only (0,3,0) and (0,2,1) are substantially perturbed. These two bands are  $\Delta\nu_0 \approx 113\text{ cm}^{-1}$  apart, see the vertical arrow in Fig. 7 (upper), and therefore the level shifts have a relatively small magnitude, preserving the asymmetric top energy pattern.

For  $D_2H^+$ , both the (1,2,0) and (1,0,2) bands are close in energy ( $\Delta\nu_0 \approx 67\text{ cm}^{-1}$ ) and have symmetry  $A_1$ . Thus they

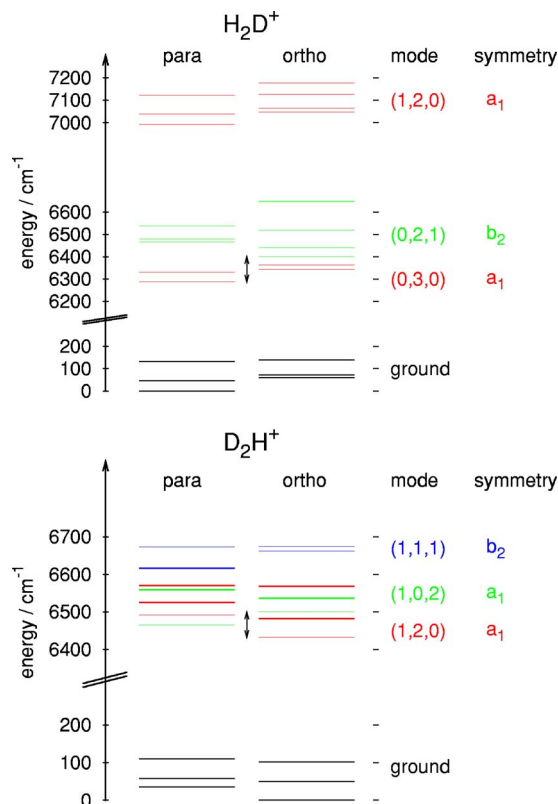


FIG. 7. (Color online) The lowest rotational levels of  $H_2D^+$  (upper) and  $D_2H^+$  (lower) for the bands of interest. The level positions are taken from the *ab initio* line list (Ref. 63) which was obtained using the methodology described in Refs. 31 and 38. For  $D_2H^+$ , the seven levels actually probed by spectroscopy (see Table II) are drawn thicker. Due to the difference in band origin of  $113\text{ cm}^{-1}$  for  $H_2D^+$  (vertical arrow), the (0,2,1) and (0,3,0) bands are only coupled by a small Coriolis effect, thus preserving the asymmetric top energy level patterns. For  $D_2H^+$ , the band origin difference for (1,0,2) and (1,2,0) is quite small ( $67\text{ cm}^{-1}$ ), leading to strong mixing by Fermi resonances.

are mixed by Fermi resonances, and therefore the vibrational assignments given in Table II have to be taken as an approximation. Based on this approximative band assignment, the degree of perturbation is more pronounced than for  $H_2D^+$ , see Fig. 7 (lower). From the simple symmetry arguments, there is also Coriolis coupling between (1,1,1) and the other two bands, although of small magnitude.

### D. Kinetic temperature of ions

The stable and reliable operation of the commercial diode lasers permitted us to measure spectroscopically several properties of the trapped ions, as, for example, their kinetic temperature. As indicated before, the measured Doppler temperature of the ions is higher than the nominal temperature of the trap. It is of special interest to determine the main influence on this discrepancy, as also discussed by Mikosch *et al.*<sup>44</sup> In particular, the influence of hot gases leaking from the ion source of the laser power and of the rf field have been tested. Applying the relation

$$\sigma_D = \sqrt{\frac{k_B T}{m c^2}} \nu_0, \quad (7)$$

the kinetic temperature  $T$  of the ions has been calculated using the ion mass  $m$  and the fitted Doppler width  $\sigma_D$ . Under



TABLE IV. Calculated and measured relative Einstein  $B_{lu}$  coefficients for several groups of transitions starting from the same rotational levels in H<sub>2</sub>D<sup>+</sup> or D<sub>2</sub>H<sup>+</sup>.

Transition	Line position (cm <sup>-1</sup> )	Laser power (mW)	Meas. $B_{lu}$	Calc. $B_{lu}$	
H <sub>2</sub> D <sup>+</sup>					
(0,3,0)	1 <sub>01</sub> ← 0 <sub>00</sub>	6330.973	4.0	0.32 ± 0.02	0.31
(0,2,1)	1 <sub>11</sub> ← 0 <sub>00</sub>	6466.532	1.8	1	1
(0,3,0)	1 <sub>10</sub> ← 1 <sub>11</sub>	6303.784	5.0	0.29	0.29
(0,2,1)	0 <sub>00</sub> ← 1 <sub>11</sub>	6340.688	5.3	0.27 ± 0.03	0.27
(0,2,1)	2 <sub>02</sub> ← 1 <sub>11</sub>	6459.036	4.1	0.35 ± 0.04	0.34
D <sub>2</sub> H <sup>+</sup>					
(1,2,0)	1 <sub>11</sub> ← 0 <sub>00</sub>	6482.033	3.8	0.33 ± 0.02	0.32
(1,0,2)	1 <sub>11</sub> ← 0 <sub>00</sub>	6536.319	1.6	1	1

normal operating conditions, the ion temperature for H<sub>2</sub>D<sup>+</sup> has been measured to be 27 ± 2 K (corresponding to  $\sigma_D \approx 150$  MHz), using the trapping parameters  $V_0 = 15$  V and  $f = 17$  MHz (see Sec. II B) and moderate laser power of 2 mW (see Fig. 4). For D<sub>2</sub>H<sup>+</sup>, the measured Doppler temperature was determined to be lower by a few kelvins. Allowing an excess of hot gas (300 K) from the source region to leak to the ion trap did not have a measurable impact on the ion temperature. This is probably due to the fact that the hot gases entering the ion trap are readily thermalized. Likewise, a pronounced heating of the ions by the laser could not be detected. A laser power in excess of 2 mW only pretended a heating effect by saturating the peak maximum and thereby apparently broadening the measured peak, giving it a non-Doppler profile. For this reason, special care was used to employ low laser power when determining the Doppler temperature. The most noticeable effect on the kinetic ion temperature was caused by the amplitude of the rf voltage. It was easy to heat the ions by using rf voltage amplitudes beyond  $V_0 = 50$  V. As an amplitude increase should not lead to higher ion temperatures in an ideal multipole trap, this effect can only be explained by imperfections (patch fields) or by a direct heating of the trap by the rf power. Still, it was difficult to obtain kinetic ion temperatures substantially below the above mentioned 27 K, even when approaching the lowest possible rf amplitudes of about  $V_0 = 10$  V. Thus, there is a discrepancy of about 10 K to the nominal trap temperature of 17 K.

Numerical three-dimensional simulations of a single ion moving in the 22-pole trap were performed to attempt resolving this discrepancy. These computations take into account the combined effects of the elastic collisions with the He buffer gas, the perfect rf multipole field, as well as the electrostatic field of the endelectrodes.<sup>65</sup> Space charge effects were neglected due to the low number of stored ions. Similar calculations for other types of multipole traps have been presented by Gerlich.<sup>58</sup> As pointed out in that work, the rf field of a multipole trap conserves the energy of the ion after reflection from the effective rf walls, and it is only by including buffer gas collisions that heating effects occur. These heating effects depend on the trap geometry and multipolarity, the rf frequency, and also on the ion-neutral mass ratio. Preliminary results of our simulations thus show that a tem-

perature increase of about 2 K can be explained by collisions of the H<sub>2</sub>D<sup>+</sup> ions with the He buffer in the rf field, and a further 2 K increase can be expected when the influence of the electrostatic field of the endelectrodes (shown in the inset in Fig. 2) is included into the simulations. This relatively small heating effect is due to the favorable ion-neutral mass ratio, in contrast to an unfavorable case as, for example, H<sub>3</sub><sup>+</sup>+Ar, where a pronounced heating effect has been observed.<sup>44</sup> In summary, only about half of the temperature discrepancy of 10 K can be explained by the operation of a perfect ion trap, while the remaining temperature increase is probably caused by trap imperfections or potential distortion,<sup>44,58</sup> but also the kinetic energy release in exothermic exchange reactions with *o*-H<sub>2</sub> (or traces of HD or D<sub>2</sub>) could play a role.

### E. Measurement of relative Einstein $B_{lu}$ coefficients

Tables I–III list the *ab initio* calculated coefficients  $A_{ul}$  for spontaneous emission for all transitions. In laser probe experiments such as LIR, the quantity of interest is the coefficient for laser absorption, the Einstein  $B_{lu}$  coefficient, which can be obtained using

$$B_{lu} = \frac{g_u}{g_l} \frac{c^3 A_{ul}}{8\pi h \nu^3}, \quad (8)$$

where  $g_u$  and  $g_l$  are the rotational degeneracies  $g = 2J + 1$  of the upper and lower states. These calculated  $B_{lu}$  coefficients are also included in the tables, and for simplicity they have been normalized to the respective strongest transitions for H<sub>2</sub>D<sup>+</sup> and D<sub>2</sub>H<sup>+</sup>.

If one wants to measure the rotational level population of a molecular species, it is important to know how reliable the predictions for the (relative)  $B_{lu}$  coefficients are. The simple fact that all *ab initio* predicted lines have been found in this search gave us the confidence that the calculated  $B_{lu}$  coefficients are relatively correct within, say, a factor of 2. To get a more quantitative picture, relative  $B_{lu}$  coefficients have been measured using transitions in H<sub>2</sub>D<sup>+</sup> and D<sub>2</sub>H<sup>+</sup> starting from the same rotational level. Special care has been taken in these measurements not to saturate the signals by applying too much laser power, thereby probably skewing the ratios. Table IV gives an overview of the measurements where

groups of relatively strong transitions have been selected to compare the measured relative coefficient  $B_{lu}$  to the calculated ones. With the stable and computer-controlled diode lasers, these measurements could be done in an automated fashion: The laser was tuned iteratively to the maximum of the respective peaks, and the background-corrected counts divided by the laser power yielded the relative strength of the transition. If necessary, the slight difference in Doppler widths for distant peaks was accounted for (because it is the area and not the maximum of the peak which matters).

As seen in Table IV, the applied experimental method is able to measure the relative  $B_{lu}$  coefficients within 10% of error, as determined from several automated runs. The agreement between experiment and calculations is surprisingly good, and the different strength of the three transitions starting at the  $I_{11}$  rotational level in  $H_2D^+$  is also well reproduced. A similar good agreement within overtone/composition bands of  $D_2H^+$  has been reported by Fárník *et al.* [see their Fig. 7(b)], although statistically significant discrepancies have been found comparing the fundamental band  $\nu_1$  to overtone/composition bands in  $H_2D^+$  and  $D_2H^+$ .<sup>26</sup> Anyway, as the determination of rotational populations requires the  $B_{lu}$  coefficients to be relatively correct within the applied band, the good agreement in Table IV not only gives a solid basis for the determination of rotational populations<sup>47</sup> but also suggests that the overall reaction probability of the excited  $H_2D^+$  or  $D_2H^+$  ions with  $H_2$  does not depend on the type of combination band or rotational state. This is astonishing, as it is known that different fundamental vibrational modes can have different reaction probabilities, as is, for example, the case for  $C_2H_2^+ + H_2$ .<sup>52,53</sup> One reason of this mode independence is probably the fact that the excited states considered lie well above the reaction endothermicity of  $170\text{ cm}^{-1}$ , and that the highly excited ions have several different possibilities to react in collisions with  $H_2$  while decaying.

## V. CONCLUSIONS AND FURTHER EXPERIMENTS

The initial motivation for this research is to understand the role of the nuclear spin in low-temperature ion-molecule collisions, and thereby explain the rotational populations of ions at cryogenic temperatures and their dependence on the  $o/p$  ratio of the  $H_2$  collision partner. Such information is crucial to fully understand the processes in low-temperature interstellar clouds, in particular, deuteration processes.

The present work describes the spectroscopic tools needed to reach this final goal. Applying the method of laser induced reaction (LIR), several laser sources have been used to excite rovibrational transitions of  $H_2D^+$  and  $D_2H^+$  when embedded in cold  $n$ - $H_2$  gas. Of the hitherto used laser systems (FELIX,<sup>46,66</sup> OPO, Agilent commercial diode laser), the diode lasers are ideal to probe the level populations and to explore rate coefficients of the collision systems due to their easy computer-controlled operation and stability.

An excellent agreement between experiment and *ab initio* calculations has been observed for the line positions and (relative) Einstein  $B$  coefficients. Especially the latter fact is of paramount importance not only for the astronomical com-

munity but also when reliable rotational populations have to be determined in laser probe experiments. Such experiments, accompanied by microcanonical simulations, are currently performed at the I. Physikalisches Institut in Köln, using  $n$ - $H_2$  and  $p$ - $H_2$  as low-temperature collision partners.

## ACKNOWLEDGMENTS

This work has been financially supported by the Deutsche Forschungsgemeinschaft (DFG) via the Forschergruppe FOR 388 "Laboratory Astrophysics" and SFB494, the Nederlandse Organisatie voor Wetenschappelijk Onderzoek (NWO) via Grant No. 614.000.415, and the European QUA-SAAR network. The authors thank Wim van der Zande and Danny Ramsamoedj (Radboud Universiteit Nijmegen) for supplying parahydrogen at the initial stage of the research. Furthermore the authors acknowledge the excellent support by the electronic and mechanical workshops of Leiden University (Ewie de Kuyper, Koos Benning, René Overgaww, Arno van Amersfoort). O.A. and E.H. thank for the many discussions and hospitality of the Düsseldorf group (Andreas Wicht, Bernhard Roth), where part of this research has been conducted. S.S. thanks M. Okhupkin, A. Nevsky, B. Roth, and H. Daerr for the diode laser calibration.

<sup>1</sup>T. Oka, Phys. Rev. Lett. **45**, 531 (1980).

<sup>2</sup>C. M. Lindsay and B. J. McCall, J. Mol. Spectrosc. **210**, 60 (2001).

<sup>3</sup>D. Gerlich, E. Herbst, and E. Roueff, Planet. Space Sci. **50**, 1275 (2002).

<sup>4</sup>T. J. Millar, Space Sci. Rev. **106**, 73 (2003).

<sup>5</sup>D. C. Lis, E. Roueff, M. Gerin, T. G. Phillips, L. H. Coudert, F. F. S. van der Tak, and P. Schilke, Astrophys. J. **571**, L55 (2002).

<sup>6</sup>F. F. S. van der Tak, P. Schilke, H. S. P. Müller, D. C. Lis, T. G. Phillips, M. Gerin, and E. Roueff, Astron. Astrophys. **388**, L53 (2002).

<sup>7</sup>B. Parise, C. Ceccarelli, A. G. G. M. Tielens, E. Herbst, B. Lefloch, E. Caux, A. Castets, I. Mukhopadhyay, L. Pagani, and L. Loinard, Astron. Astrophys. **393**, L49 (2002).

<sup>8</sup>B. Parise, A. Castets, E. Herbst, E. Caux, C. Ceccarelli, I. Mukhopadhyay, and A. G. G. M. Tielens, Astron. Astrophys. **416**, 159 (2004).

<sup>9</sup>C. Ceccarelli, C. Vastel, A. G. G. M. Tielens, A. Castets, A. C. A. Boogert, L. Loinard, and E. Caux, Astron. Astrophys. **381**, L17 (2002).

<sup>10</sup>A. Bacmann, B. Lefloch, C. Ceccarelli, J. Steinacker, A. Castets, and L. Loinard, Astrophys. J. **585**, L55 (2003).

<sup>11</sup>D. R. Flower, G. Pineau des Forêts, and C. M. Walmsley, Astron. Astrophys. **427**, 887 (2004).

<sup>12</sup>M. Bogey, C. Demuynck, M. Denis, J. L. Destombes, and B. Lemoine, Astron. Astrophys. **137**, L15 (1984).

<sup>13</sup>H. E. Warner, W. T. Conner, R. H. Petrmichl, and R. C. Wods, J. Chem. Phys. **81**, 2514 (1984).

<sup>14</sup>T. Amano and T. Hirao, J. Mol. Spectrosc. **233**, 7 (2005).

<sup>15</sup>R. Stark, F. F. van der Tak, and E. F. van Dishoeck, Astrophys. J. **521**, L67 (1999).

<sup>16</sup>C. Vastel, T. G. Phillips, and H. Yoshida, Astrophys. J. **606**, L127 (2004).

<sup>17</sup>C. Ceccarelli, C. Dominik, B. Lefloch, P. Caselli, and E. Caux, Astrophys. J. **607**, L51 (2004).

<sup>18</sup>P. Caselli, F. F. S. van der Tak, C. Ceccarelli, and A. Bacmann, Astron. Astrophys. **403**, L37 (2003).

<sup>19</sup>F. van der Tak, P. Caselli, C. M. Walmsley, C. Ceccarelli, A. Bacmann, and A. Crapsi, in *The Dense Interstellar Medium in Galaxies*, edited by S. Palfzner, C. Kramer, C. Staubmeier, and A. Heithausen (Springer, Berlin, 2004), p. 549.

<sup>20</sup>J.-T. Shy, J. W. Farley, and W. H. Wing, Phys. Rev. A **24**, 1146 (1981).

<sup>21</sup>S. C. Foster, A. R. W. McKellar, I. R. Peterkin, J. K. G. Watson, F. S. Pan, M. W. Crofton, R. S. Altman, and T. Oka, J. Chem. Phys. **84**, 91 (1986).

<sup>22</sup>T. Amano and J. K. G. Watson, J. Chem. Phys. **81**, 2869 (1984).

<sup>23</sup>T. Amano, J. Opt. Soc. Am. B **2**, 790 (1985).

<sup>24</sup>K. G. Lubich and T. Amano, Can. J. Phys. **62**, 1886 (1984).

<sup>25</sup>S. C. Foster, A. R. W. McKellar, and J. K. G. Watson, J. Chem. Phys. **85**, 664 (1986).

- <sup>26</sup>M. Fárnik, S. Davis, M. A. Kostin, O. L. Polyansky, J. Tennyson, and D. Nesbitt, *J. Chem. Phys.* **116**, 6146 (2002).
- <sup>27</sup>R. Moss, *Mol. Phys.* **78**, 371 (1993).
- <sup>28</sup>V. I. Korobov, *Phys. Rev. A* **74**, 052506 (2006).
- <sup>29</sup>B. Roth, J. C. J. Koelemeij, H. Daerr, and S. Schiller, *Phys. Rev. A* **74**, 040501 (2006).
- <sup>30</sup>J. C. J. Koelemeij, B. Roth, A. Wicht, I. Ernsting, and S. Schiller, *Phys. Rev. Lett.* **98**, 173002 (2007).
- <sup>31</sup>J. Ramanlal and J. Tennyson, *Mon. Not. R. Astron. Soc.* **354**, 161 (2004).
- <sup>32</sup>O. L. Polyansky, A. G. Császár, S. V. Shirin, N. F. Zobov, P. Barletta, J. Tennyson, D. W. Schwenke, and P. J. Knowles, *Science* **299**, 539 (2003).
- <sup>33</sup>J. Tennyson, P. Barletta, M. A. Kostin, O. L. Polyansky, and N. F. Zobov, *Spectrochim. Acta, Part A* **58**, 663 (2002).
- <sup>34</sup>W. Cencek, J. Rychlewski, R. Jaquet, and W. Kutzelnigg, *J. Chem. Phys.* **108**, 2831 (1998).
- <sup>35</sup>J. Tennyson and O. L. Polyansky, *Phys. Rev. A* **50**, 314 (1994).
- <sup>36</sup>B. M. Dinelli, C. R. Le Sueun, J. Tennyson, and R. D. Amos, *Chem. Phys. Lett.* **232**, 295 (1995).
- <sup>37</sup>R. Röhse, W. Kutzelnigg, R. Jaquet, and W. Klopper, *J. Chem. Phys.* **101**, 2231 (1994).
- <sup>38</sup>O. L. Polyansky and J. Tennyson, *J. Chem. Phys.* **110**, 5056 (1999).
- <sup>39</sup>R. Moss, *Mol. Phys.* **89**, 195 (1996).
- <sup>40</sup>P. Hlavenka, R. Plašil, G. Bánó, I. Korolov, D. Gerlich, J. Ramanlal, J. Tennyson, and J. Glosík, *Int. J. Mass. Spectrom.* **255–256**, 170 (2006).
- <sup>41</sup>L. Kao, T. Oka, S. Miller, and J. Tennyson, *Astrophys. J., Suppl. Ser.* **77**, 317 (1991).
- <sup>42</sup>L. Neale, S. Miller, and J. Tennyson, *Astrophys. J.* **464**, 516 (1996).
- <sup>43</sup>J. Ramanlal, Ph.D. thesis, University of London, 2004.
- <sup>44</sup>J. Mikosch, H. Kreckel, R. Wester, R. Plašil, J. Glosík, D. Gerlich, D. Schwalm, and A. Wolf, *J. Chem. Phys.* **121**, 11030 (2004).
- <sup>45</sup>J. Glosík, P. Hlavenka, R. Plašil, F. Windisch, D. Gerlich, A. Wolf, and H. Kreckel, *Philos. Trans. R. Soc. London, Ser. A* **364**, 2931 (2006).
- <sup>46</sup>*Astrochemistry: Recent Successes and Current Challenges*, Proceedings of the 231st Symposium of the International Astronomical Union, Pacific Grove, California, USA, 29 August-2 September 2005, edited by D. C. Lis, G. A. Blake, and E. Herbst (Cambridge University Press, Cambridge, 2006).
- <sup>47</sup>O. Asvany, E. Hugo, and S. Schlemmer (unpublished).
- <sup>48</sup>O. Asvany, Padma Kumar P, B. Redlich, I. Hegemann, S. Schlemmer, and D. Marx, *Science* **309**, 1219 (2005).
- <sup>49</sup>S. Schlemmer and O. Asvany, *J. Phys.: Conf. Ser.* **4**, 134 (2005).
- <sup>50</sup>S. Borman, *Chem. Eng. News* **83**, 45 (2005).
- <sup>51</sup>S. Schlemmer, T. Kuhn, E. Lescop, and D. Gerlich, *Int. J. Mass. Spectrom.* **185**, 589 (1999).
- <sup>52</sup>S. Schlemmer, E. Lescop, J. v. Richthofen, and D. Gerlich, *J. Chem. Phys.* **117**, 2068 (2002).
- <sup>53</sup>S. Schlemmer, O. Asvany, and T. Giesen, *Phys. Chem. Chem. Phys.* **7**, 1592 (2005).
- <sup>54</sup>O. Asvany, T. Giesen, B. Redlich, and S. Schlemmer, *Phys. Rev. Lett.* **94**, 073001 (2005).
- <sup>55</sup>I. N. Kozin, O. L. Polyansky, and N. F. Zobov, *J. Mol. Spectrosc.* **128**, 126 (1988).
- <sup>56</sup>N. G. Adams and D. Smith, *Astrophys. J.* **248**, 373 (1981).
- <sup>57</sup>D. Gerlich, *Phys. Scr., T* **59**, 256 (1995).
- <sup>58</sup>D. Gerlich, in *Advances in Chemical Physics: State-Selected and State-to-State Ion-Molecule Reaction Dynamics*, edited by C.-Y. Ng and M. Baer (Wiley, New York, 1992), vol. LXXXII, pp. 1–176.
- <sup>59</sup>L. S. Rothman *et al.*, *J. Quant. Spectrosc. Radiat. Transf.* **96**, 139 (2005).
- <sup>60</sup>O. Asvany, E. Hugo, and S. Schlemmer, *J. Vac. Sci. Technol. A* **25**, 628 (2007).
- <sup>61</sup>F. Müller, G. von Basum, A. Popp, D. Halmer, P. Hering, M. Mürtz, F. Kühnemann, and S. Schiller, *Appl. Phys. B: Lasers Opt.* **80**, 307 (2005).
- <sup>62</sup>J. Tennyson, M. A. Kostin, P. Barletta, G. J. Harris, J. Ramanlal, O. L. Polyansky, and N. F. Zobov, *Comput. Phys. Commun.* **163**, 85 (2004).
- <sup>63</sup>The full electronic lists of H<sub>2</sub>D<sup>+</sup> and D<sub>2</sub>H<sup>+</sup> transitions are not published, but can be obtained from Jonathan Tennyson.
- <sup>64</sup>H. Kreckel, J. Tennyson, D. Schwalm, D. Zajfman, and A. Wolf, *New J. Phys.* **6**, 151 (2004).
- <sup>65</sup>O. Asvany and S. Schlemmer (unpublished).
- <sup>66</sup>D. Oepts, A. van der Meer, and P. van Amersfoort, *Infrared Phys. Technol.* **36**, 297 (1995).